https://doi.org/10.5194/acp-2021-527
Preprint. Discussion started: 6 July 2021


Atmospheric Chemistry and Physics Discussions

# Technical note: Quality assessment of ozone reanalysis products over subarctic Europe for biome modeling and ozone risk mapping

Stefanie Falk[1], Ane Victoria Vollsnes[2], Aud Eriksen[2], Frode Stordal[1], and Terje Koren Berntsen[1]

[1]Department of Geosciences, University of Oslo, Oslo, Norway
[2]Department of Biosciences, University of Oslo, Oslo, Norway

**Correspondence:** Stefanie Falk (stefanie-elfriede.falk@gmx.net)

**Abstract.** We assess the quality of regional or global ozone reanalysis data for biome modeling and ozone ($O_3$) risk mapping over subarctic Europe where monitoring is sparse. Reanalysis data can be subject to systematic errors originating from, e.g., quality of assimilated data, distribution and strength of precursor sources, incomprehensive atmospheric chemistry or land–atmosphere exchange, and spatiotemporal resolution. Here, we evaluate three selected global and regional ozone reanalysis products. Our analysis suggests that global reanalysis products do not reproduce observed ground-level ozone well in the subarctic region. Only the Copernicus Atmosphere Monitoring Service Regional Air Quality (CAMSRAQ) reanalysis ensemble sufficiently captures the observed seasonal cycle. We computed the root mean square error (RMSE) by season. The RMSE variation between $(2.6-6.6)\,\mathrm{ppb}$ suggests inherent challenges even for the best reanalysis product (CAMSRAQ). $O_3$ concentrations in the region are systematically underestimated by $(2-6)\,\mathrm{ppb}$ compared to the tropospheric background ozone concentrations derived from observations. Furthermore, we explore the suitability of the CAMSRAQ for gap-filling at one site in northern Norway with a long-term record but not belonging to the observational network. We devise a reconstruction method based on Reynolds decomposition and adhere to recommendations by the United Nations Economic Commission for Europe (UNECE) Long Range Transboundary Air Pollution (LRTAP) convention. The thus reconstructed data for two weeks in July 2018 are compared with CAMSRAQ evaluated at the nearest neighboring grid point. Our reconstruction method performs better ($78\,\%$ accuracy) than CAMSRAQ ($73\,\%$ accuracy) but diurnal extremes are underestimated by both.

## 1 Introduction

Tropospheric ozone ($O_3$) as a secondary pollutant is highly toxic and harmful to human health (WHO - World Health Organization, 2008; Fleming et al., 2018) and a variety of ecosystems globally (Mills et al., 2011, 2018; Emberson, 2020). At the same time $O_3$ is acting as a potent greenhouse gas (Myhre et al., 2013). Ozone causes an estimated annual global yield loss of four major crops (wheat, rice, maize, and soybean) of $3-15\,\%$ (Ainsworth, 2017) and threatens food security in rapidly developing countries, e.g., in East and South-East Asia (Tang et al., 2013; Tai et al., 2014; Chuwah et al., 2015; Mills et al., 2018).

In the troposphere, $O_3$ is produced in complex chemical cycles involving precursors such as carbon monoxide (CO) and hydrocarbons (e.g. methane, terpenes) in the presence of nitrogen oxides ($NO_x$) (Monks et al., 2015). These hydrocarbons

https://doi.org/10.5194/acp-2021-527
Preprint. Discussion started: 6 July 2021


Atmospheric Chemistry and Physics Discussions

can be of anthropogenic or natural origin and are often referred to as volatile organic compounds (VOCs) and biogenic VOCs (BVOCs), respectively. The primary sink of $O_3$ in the troposphere is dry deposition to different surfaces of which the removal by vegetation amounts to over $50\,\%$ (Monks et al., 2015; Clifton et al., 2020). Plants take up $O_3$ through their stomata (leaf openings for gas exchange). In the leaf interior, $O_3$ induced radical oxygen species (ROS) damage cell membranes leading to necrosis and ultimately to programmed cell death (Kangaskärvi et al., 2005). Ozone damage is considered to accumulate over time. To assess the potential risk posed by ozone, various metrics have been defined. Mills et al. (2011) showed that the Phytotoxic Ozone Dose over a threshold y ($\mathrm{POD_y}$) (integrated flux through the stomata) is capable of capturing observed negative effects on crops and semi-natural vegetation (e.g. clover) better than an integrated exceedance over a fixed concentration threshold (e.g. $40\,\mathrm{ppb}$). Furthermore, $O_3$ uptake and subsequent damage negatively affect photosynthesis and stomatal conductance (e.g., Pellegrini et al., 2011; Watanabe et al., 2014). This, in turn, reduces gross primary production (GPP) (Lombardozzi et al., 2015b, a; Hoshika et al., 2015) and has the potential to off-set growth effects of carbon dioxide ($CO_2$) fertilization in the future (Franz and Zaehle, 2021) as well as to induce measurable positive feedback on surface temperatures in highly polluted regions (Zhu et al., 2021).

Due to these risks, $O_3$ is included in air quality monitoring networks under the WMO (World Meteorological Organization) Global Atmosphere Watch (GAW) program. Remote regions in the Arctic and subarctic, however, are scarcely covered (refer to Section 2 for the coverage of northern Fennoscandia). With climate change already promoting an earlier and longer growing season (Linderholm, 2006; Karlsen et al., 2007; Høgda et al., 2013), subarctic vegetation may become more vulnerable to damage induced by cumulative $O_3$ uptake in the future. Although, species acclimated to the Arctic and subarctic climates were not found to be more sensitive to ozone than species in less extreme environments (Karlsson et al., 2021).

$O_3$ as well as its precursors is subject to atmospheric transport causing pollution peaks in the otherwise pristine Arctic and subarctic environments (Stevenson et al., 2005; Young et al., 2013). This long-range transport of pollutants has been identified as one of the main sources of enhanced $O_3$ concentration ($[O_3]$) in Fennoscandia (Andersson et al., 2017). Peak $[O_3]$ in summer is often a combination of stagnant weather situations accompanied by heatwaves and enhanced precursor emissions due to extensive forest fires (e.g. in 2003, 2006, 2018) (Lindskog et al., 2007; Karlsson et al., 2013). The prominently elevated $[O_3]$ which occurs in April/May over northern Fennoscandia is caused by other factors. This so-called ozone spring peak can be attributed to a build-up of $O_3$ and precursors due to a suppression of removal from the troposphere during the polar night and their photo-chemical reactivation come spring (Monks, 2000). Tropopause folding events are another contributor and cause an intrusion of dry and $O_3$ rich air masses from the stratosphere (Škerlak et al., 2015).

As indicated above, $\mathrm{POD_y}$ is an integrated $O_3$-flux quantity. A proper assessment of $\mathrm{POD_y}$ relies on a set of complete, 1-hourly meteorological and ozone data. Since gaps in observational data are common, many techniques of varying complexity have been devised for filling these. The applicability often depends on the shape of the variables' signal, e.g. prominence of the diurnal cycle. In the simplest case of monotonously increasing/decreasing data and little fluctuation, a first-order polynomial may suffice. In the following, we give an account of the detailed practical recommendations by Mills et al. (2020). For gaps of less than $5\,\mathrm{h}$, gap-filling with an average value over the preceding and subsequent time steps is recommended. This method, however, does not suffice for observables such as $O_3$ that display a distinct diurnal cycle and leads to an underestimation around

https://doi.org/10.5194/acp-2021-527
Preprint. Discussion started: 6 July 2021


Atmospheric Chemistry and Physics Discussions

noon and an overestimation during the night, respectively. Similarly, gaps longer than $5\,\mathrm{h}$ but less than $24\,\mathrm{h}$ ought to be filled by averaging the preceding and subsequent day at each time step. For gaps exceeding $1\,\mathrm{d}$, Mills et al. (2020) suggest exploiting data from close-by monitoring stations with a Pearson correlation coefficient $r^2$ of preferably $0.6$ or higher. A period of at least one season ($3\,\mathrm{months}$) is recommended for this statistical analysis. To account for the seasonal variability, the projection between sites is to be computed for the same season the gap occurred. Where available, auxiliary data from model reanalysis can be used.

As indicated above, reanalysis data can be used for gap-filling, but more often it is used to study emerging trends in tropospheric ozone in remote regions such as the Arctic and subarctic, where scarce observations have to be supplemented with model simulations. Atmospheric reanalyses are based on a fixed state of an operational data assimilation system used for forecasts ingested with the most complete set of observational data. In terms of atmospheric chemistry, this includes meteorological data as well as observations of chemical substances from, e.g., satellite, airborne instruments, and ground-level monitoring station networks. Global reanalyses, however, have already been shown to underestimate $[\mathrm{O_3}]$ particularly over the polar region (Huijnen et al., 2020; Barten et al., 2020). Barten et al. (2020) suggest, that global reanalysis products that only assimilate satellite products do not sufficiently cover $[\mathrm{O_3}]$ variations. The large discrepancies can be explained by the low spatiotemporal resolution not capturing atmospheric boundary layer dynamics and missing processes such as a mechanistic ocean–atmosphere $\mathrm{O_3}$ exchange.

In the following, we evaluate and validate the quality of three reanalysis products concerning surface ozone over northern Fennoscandia with available long-term observations. All data are presented in Section 2. In Section 3, we derive a generalized ozone climatology for northern Fennoscandia from in situ observations and quantify the overall quality of the ozone reanalysis. Based on these results, we provide a methodology for reconstructing missing observational data over an extended period of several weeks based on Reynolds decomposition and compare it with the evaluation of the best reanalysis product at the nearest neighboring grid point. We close with discussions and conclusions (Section 4).

## 2 Data

In this section, we present long-term ground-level $\mathrm{O_3}$ observation data for our target region, northern Fennoscandia, which we define here as north of $67.5\,^{\circ}\mathrm{N}$, and determine their correlation. To this end, we compute Pearson correlation coefficients pair-wise. All observational data are taken from the EBAS atmospheric database operated by the Norwegian Institute for Air Research (NILU). We also present the selected ozone reanalysis products provided by the European Centre for Medium-Range Weather Forecasts (ECMWF) and the Copernicus Atmospheric Monitoring Service (CAMS).

### 2.1 Ozone monitoring sites

Northern Fennoscandia is sparsely covered by sites that monitor tropospheric background $[\mathrm{O_3}]$ and report to the EBAS atmospheric database (Fig. 1). A detailed overview over the past and present ozone monitoring sites in northern Fennoscandia with a considerable duration of data acquisition is given in Table 1. Continuous ozone data are available as early as mid-1986 from

https://doi.org/10.5194/acp-2021-527
Preprint. Discussion started: 6 July 2021


Atmospheric Chemistry and Physics Discussions

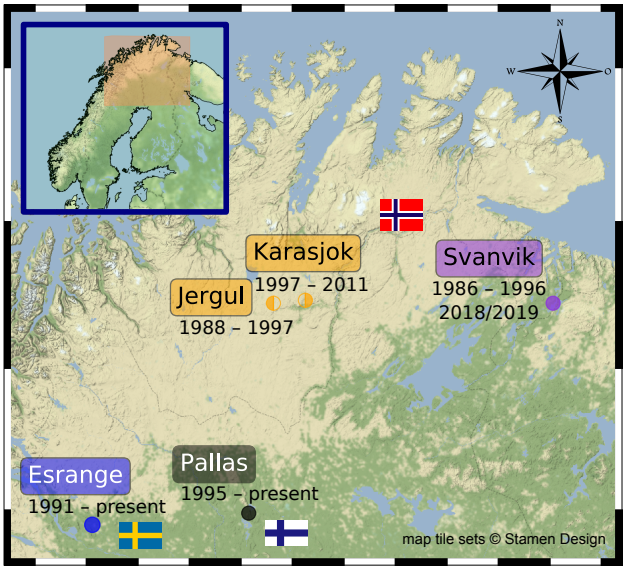


**Figure 1.** Subarctic Europe north of $67.5\,^{\circ}\mathrm{N}$, here referred to as northern Fennoscandia. Locations of past and present ozone observation sites used in this study. For more details see Table 1. The introduced color coding for the monitoring sites is used throughout.

the NILU atmospheric monitoring site at Svanvik located in the Pasvik valley. Data taking, however, did not continue after 1996. To supplement field experiments on subarctic vegetation, we installed an ozone monitor at Svanvik exclusively for the growing seasons 2018/19 in collaboration with NILU. Due to irregularities in data acquisition, two weeks' worth of data is missing from the record in July 2018. These shall be subject to our proposed data reconstruction (Section 3.2). At the same latitude but further west, a station was established in the early 1990s above the Karasjohka river valley. Originally placed at Jergul the station was later moved downstream closer to the city of Karasjok using the same equipment but increasing the recorded floating-point precision of the ozone monitor. The station was decommissioned in 2011. Data series from Svanvik and Jergul are highly uncertain because of insufficient quality control and irregular calibration before 1997 which led to degradation of the monitors over time and introduced drifts in the ozone data series (Solberg, 2003). Solberg (2003) further reported a systematic uncertainty for these data of the order of $10\,\%$, which they deemed too large to conduct a strict trend analysis of tropospheric background $[\mathrm{O_3}]$. For our purpose of evaluating seasonal cycles on a climatological timescale, we can consider these uncertainties as small enough. Further south, two stations have been established at Esrange (Sweden) and Pallas (Finland) in the early 1990s. Data are available from EBAS until the end of 2018 and 2019, respectively (last accessed April 2021).

In Fig. 2, daily mean ozone concentration climatologies ($\langle[\mathrm{O_3}]\rangle$) for the data taken at Esrange, Jergul/Karasjok, Pallas, and Svanvik are shown together with their respective standard error ($\sigma_{\langle[\mathrm{O_3}]\rangle} = \frac{\sigma_{[\mathrm{O_3}]}}{\sqrt{n}}$). The annual average $\langle[\mathrm{O_3}]\rangle$ at Svanvik is $6.6\,\mathrm{ppb}$ lower compared to the other sites. This can be attributed to the station's location at lower altitude and amidst agriculturally used land surrounded by forests in contrast to Pallas where the vegetation consists of low vascular plants, mosses, and lichen (Hatakka et al., 2003). An increase in tropospheric background $[\mathrm{O_3}]$ since the early 1990s cannot be dismissed.

https://doi.org/10.5194/acp-2021-527
Preprint. Discussion started: 6 July 2021


Atmospheric Chemistry and Physics Discussions

**Table 1.** Past and present ozone observation sites in northern Fennoscandia. Data available from EBAS.

| Name | Country | ID | Location | | | Operational |
|---|---|---|---|---|---|---|
| | | | lat (°N) | lon (°E) | alt (m) | |
| Esrange | SWE | SE0013R | 67.83 | 21.07 | 475 | 1991 – 2018† |
| Jergul | NOR | NO0030R | 69.45 | 24.60 | 255 | 1997 – 2011 |
| Karasjok | NOR | NO0055R | 69.467 | 25.217 | 333 | 1988 – 1997 |
| Pallas | FIN | FI0096G | 67.97 | 24.12 | 565 | 1995 – 2019† |
| Svanvik | NOR | NO0047R | 69.45 | 30.03 | 30 | 1986 – 1996‡ |

† Data availability on EBAS at present.
‡ Exclusive monitoring in growing season 2018/19.

Given 2019 was a climatologically normal year, we estimate the deviation from the 1990s ozone climatology at Svanvik $\delta[O_3] = (1.2 \pm 5.0)\,\mathrm{ppb}$. The $\delta[O_3]$ indicates a small and statistically insignificant increase in $[O_3]$.

The Pearson correlation coefficients ($r^2$) for the combined data set of Jergul/Karasjok show a high correlation with Esrange ($r^2 = 0.78$) as well as Pallas ($r^2 = 0.79$). We, therefore, combine observational data from Esrange, Jergul/Karasjok, and Pallas to derive a generalized ozone climatology for northern Fennoscandia which represents the expected tropospheric background in this region. The correlation of Svanvik with Esrange is fair ($r^2 = 0.42$), but good with Pallas ($r^2 = 0.61$). The climatologies displayed in Fig. 2 cover the known features of the ozone seasonal cycle in northern Fennoscandia well and reflect the expected increase of ozone abundance with altitude where Pallas is located at the highest altitude and Svanvik at the lowest. The highest average ozone concentration ($\langle[O_3]\rangle_{\max} = (46.35 \pm 0.17)\,\mathrm{ppb}$) is regularly observed in April/May and the lowest average concentration is reached in August/September ($\langle[O_3]\rangle_{\min} = (24.18 \pm 0.18)\,\mathrm{ppb}$). The $\sigma_{\langle[O_3]\rangle}$ lie well below $0.5\,\mathrm{ppb}$ for Esrange, Jergul/Karasjok, and Pallas. This is considerably lower than at Svanvik ($0.3\,\mathrm{ppb} < \sigma_{\langle[O_3]\rangle} \leq 1\,\mathrm{ppb}$) and can be attributed to the length of these time series, a better quality control, and less diurnal variability at higher altitudes.

### 2.2 Ozone reanalysis

There are two global reanalysis products available from ECMWF that include atmospheric tracers, including ozone, the Monitoring Atmospheric Composition and Climate (MACC) and the latest Copernicus Atmosphere Monitoring Service reanalysis (CAMSRA) (Inness et al., 2013, 2019). The temporal, as well as spatial resolution of these reanalysis products is rather coarse: 3-hourly and $0.75° \times 0.75°$ or roughly $29.3\,\mathrm{km} \times 83.4\mathrm{km}$ at the location of Svanvik. From the Copernicus Atmospheric Monitoring Service Regional Air Quality (CAMSRAQ) system, surface ozone reanalysis ensemble means are available for a European domain. The CAMSRAQ is based on nine European state-of-the-art numerical air quality models. The ensemble mean is at higher spatial and temporal resolution compared to the global reanalyses: $0.1° \times 0.1°$ (roughly $3.9\,\mathrm{km} \times 11.1\,\mathrm{km}$ at Svanvik) and 1-hourly. The periods covered differ but no data is available before the turn of the millennium. The CAMSRA is available in near real-time and covers a period of sufficient length for climate analysis (2003 – present). For this study, a shorter

https://doi.org/10.5194/acp-2021-527
Preprint. Discussion started: 6 July 2021


Atmospheric Chemistry and Physics Discussions

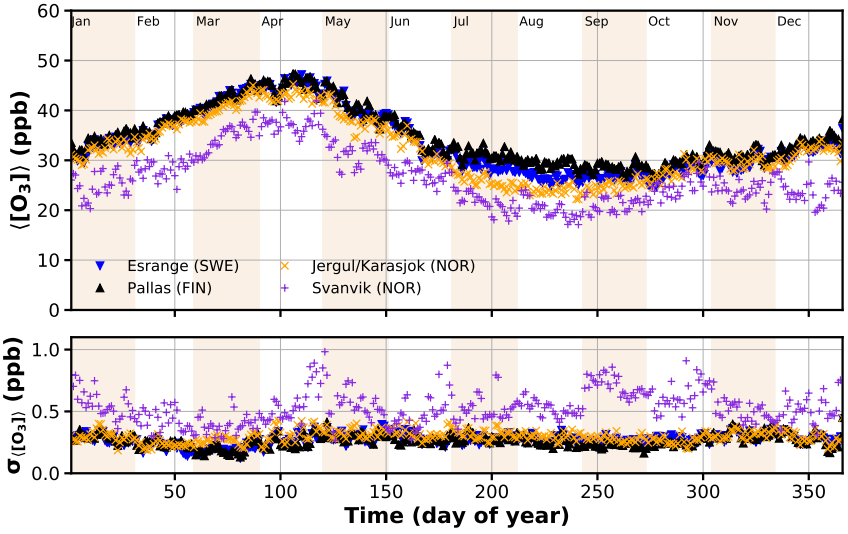


**Figure 2.** Daily mean ozone climatologies (upper panel) and standard error (lower panel) over the day of the year. All stations located in northern Fennoscandia with data records exceeding 10 years are displayed. The data taken at Jergul and Karasjok have been combined for this figure. The magnitude of the annual average $[O_3]$ reflects the hierarchy in altitude, with Pallas on top and Svanvik 6.6. ppb lower. A larger $\sigma_{\langle[O_3]\rangle}$ at Svanvik, is partly attributable to the shorter time series and systematic uncertainties due to the lack of sufficient data quality procedures. All $\langle[O_3]\rangle$ display known features of the ozone seasonal cycle in northern Fennoscandia with peak values in spring and a minimum in late summer.

subset of CAMSRA (2003–2012) has been chosen for comparability with the MACC reanalysis in terms of statistical uncertainties. The CAMSRAQ system is predominately used for air quality forecasting and the reanalysis has currently not been extended beyond 2018. All reanalyses use different but, at that time, the latest version of the operational weather forecast system (OpenIFS) from ECMWF to force their models. They differ substantially in the assimilated observational ozone data. The MACC reanalysis assimilates only satellite-derived tropospheric column ozone, while CAMSRA also includes ozone profiles from satellite retrievals. In situ observations from ozone near-surface station networks are only assimilated in the CAMSRAQ reanalysis ensemble. All relevant details concerning the reanalysis data sets are listed in Table 2.

## 3 Analysis

In the following, we assess the quality of the reanalysis products, MACC, CAMSRA, and CAMSRAQ, with respect to the generalized ozone climatology derived from ground-level ozone observations in northern Fennoscandia. We focus in particular on the seasonal cycle of $[O_3]$ with its prominent peak in spring and dip in late summer and identify the reanalysis product that best reproduces these features. We then devise a reconstruction method for missing data applicable for extended periods of

https://doi.org/10.5194/acp-2021-527
Preprint. Discussion started: 6 July 2021


Atmospheric Chemistry and Physics Discussions

**Table 2.** Global/regional ozone reanalysis products used in this study.

| Name | Provider | Resolution | | Time period | Meteorological forcing | $O_3$ assimilation |
|---|---|---|---|---|---|---|
| | | spatial | temporal | | | |
| MACC | ECMWF | $0.75° \times 0.75°$ | 3-hourly | 2003 – 2012 | OPS | satellite $^{\triangledown}$ |
| CAMSRA | ECMWF | $0.75° \times 0.75°$ | 3-hourly | 2003 – 2012 $^{\dagger}$ | ERA5 / OPS $^{\ddagger}$ | satellite $^{\blacktriangledown}$ |
| CAMSRAQ | Copernicus | $0.1° \times 0.1°$ | 1-hourly | 2014 – 2018 $^{\dagger}$ | OPS $^{\star}$ | in situ $^{\triangle}$ |

$^{\dagger}$ Subset of reanalysis data used in this study. $^{\ddagger}$ ERA5 (2003–2016), OPS (later); $^{\star}$ EURAD uses WRF for downscaling of operational IFS; $^{\triangledown}$ MLS, OMI - tropospheric column; $^{\blacktriangledown}$ SCIAMACHY, MIPAS, MLS, OMI, GOME2, SBUV2 - tropospheric column + profile; $^{\triangle}$ METEO France NRT.

data gaps based on Reynolds decomposition and compare with the best reanalysis product evaluated at the nearest neighboring grid point of Svanvik.

### 3.1 Quality of ozone reanalysis product in northern Fennoscandia

First, we evaluate the reanalysis products qualitatively at the site level. We compare the seasonal cycle of the generalized ozone climatology with seasonal cycles derived for each reanalysis product at the nearest neighboring grid point of the actual monitoring sites. In this way, we can also test the vertical resolution of the products concerning the expected ozone abundance in response to differing ground-level altitudes. The generalized ozone climatology and its respective standard deviation (gray band) shown in Fig. 3 are based on a spline fitted through the climatological daily mean $[O_3]$. The global products (MACC, CAMSRA) do not reproduce the observed seasonality of ground-level $[O_3]$ well. The MACC reanalysis (Fig. 3a) reveals a strong negative deviation (bias) amounting to $-(9 \pm 7)\,\mathrm{ppb}$ on average and displays no distinct seasonal cycle. The ozone climatology is rather flat throughout the whole cycle with a small peak in March. MACC $[O_3]$ is considerably too low compared to the generalized climatology. The March peak is followed by a flattening and a second peak in July. The seasonal low is shifted towards November/December. Also, CAMSRA matches the observed ozone climatology poorly (Fig. 3b). Despite reproducing $[O_3]$ well during the growing season (May–October), it still does not reproduce the actual seasonality in northern Fennoscandia. The CAMSRA derived spring peak lags behind observations by $1\,\mathrm{month}$ and is $5\,\mathrm{ppb}$ too low, whereas the minimum occurs in January compared to August/September. In general, CAMSRA fails in reproducing $[O_3]$ in all seasons but summer. The annual amplitude ($(26 \pm 1)\,\mathrm{ppb}$) is larger than in the climatology derived from observations ($19\,\mathrm{ppb}$). Both global reanalysis products place the $O_3$ abundance evaluated at the location of Svanvik highest. This indicates an insufficient vertical resolution of these models. This is important in terms of usage for gap-filling as well as Europe-wide or global risk assessment concerning the Arctic and subarctic vegetation that may rely on these data. In contrast, the ensemble mean of the CAMSRAQ reproduces the seasonal cycle in northern Fennoscandia well (Fig. 3c). CAMSRAQ also correctly depicts $[O_3]$ at Svanvik lower than at the other sites most likely due to the higher resolution and data assimilation of in situ ozone observation. On average, CAMSRAQ slightly underestimates $[O_3]$ ($-(2.8 \pm 0.5)\,\mathrm{ppb}$) compared to observation.

https://doi.org/10.5194/acp-2021-527
Preprint. Discussion started: 6 July 2021


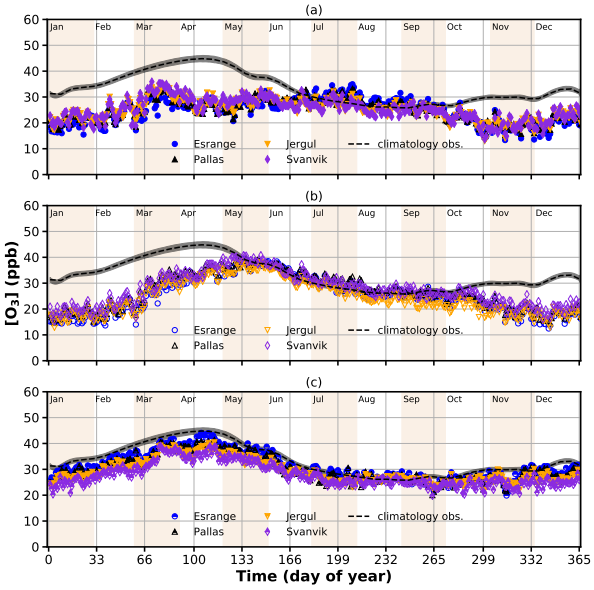


**Figure 3.** Daily mean ozone climatologies computed from the ozone reanalysis products (a) MACC; (b) CAMSRA; (c) CAMSRAQ ensemble mean. The reanalysis products were evaluated at the nearest neighboring grid point of the featured monitoring sites to assess also the vertical resolution. The generalized ozone climatology shown as gray band represents the expected seasonal cycle of tropospheric ozone background $O_3$ in northern Fennoscandia. The global products ((a), (b)) do not reproduce the observed ground-level ozone seasonality well. Their spatial resolution is too low to reproduce the station hierarchy in terms of altitude. On average, all reanalysis products display too low $[O_3]$.

In Fig. 4, we show the seasonally averaged divergence between each reanalysis product and the generalized ozone climatology which represents the expected tropospheric ozone background over the whole region. We computed the root mean square error (RMSE) for each product over land-only and display the result in the upper left corner of the respective panel. The global reanalysis products, MACC and CAMSRA (Fig. 4a,b), show large negative deviations ($\Delta[O_3] < -10\,\mathrm{ppb}$) especially in winter (DJF) and spring (MAM). The respective RSMEs range between $(12.3 - 15.2)\,\mathrm{ppb}$ (MACC) and $(10.1 - 15.6)\,\mathrm{ppb}$ (CAMSRA). We identify the smallest deviation ($\Delta[O_3] > -4\,\mathrm{ppb}$) in summer (JJA). In Summer, the MACC reanalysis deviations are overall negative except for a small region east of Tromsø were $\Delta[O_3]$ are slightly positive ($\mathrm{RSME} = 3.9\,\mathrm{ppb}$). CAMSRA ($\mathrm{RSME} = 3.6\,\mathrm{ppb}$) shows a distinctive gradient from the Norwegian coast in the west towards areas east of the Scandinavian Mountains in all seasons but summer. The deviation from the generalized ozone climatology is large and amounts to $30 - 50\,\%$ of the annual average ($\langle[O_3]\rangle = 33.3\,\mathrm{ppb}$). CAMSRAQ is shown in Fig. 4c. The white areas at the northern and eastern border represent the domain borders. The divergence from the generalized ozone climatology is considerably smaller than for the global reanalysis products and stays below $20\,\%$ ($\mathrm{RSME} \leq 6.6\,\mathrm{ppb}$) at all times. The largest deviations are again found in winter and spring, while the smallest occur in summer ($\mathrm{RSME} \leq 2.6\,\mathrm{ppb}$)).

https://doi.org/10.5194/acp-2021-527
Preprint. Discussion started: 6 July 2021


Atmospheric Chemistry and Physics Discussions

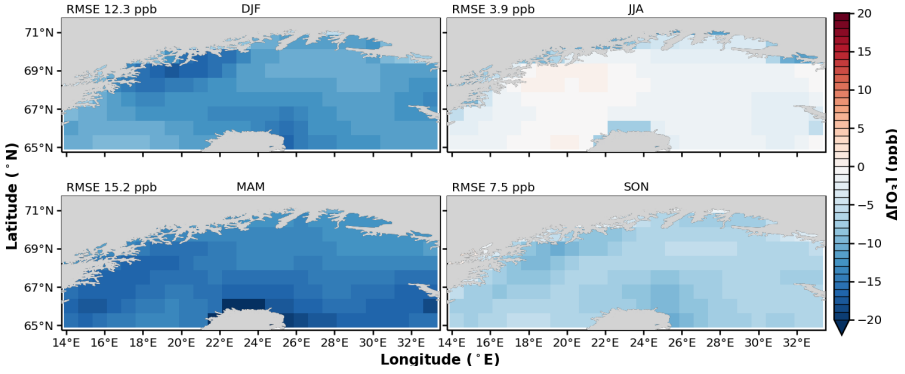


(a)

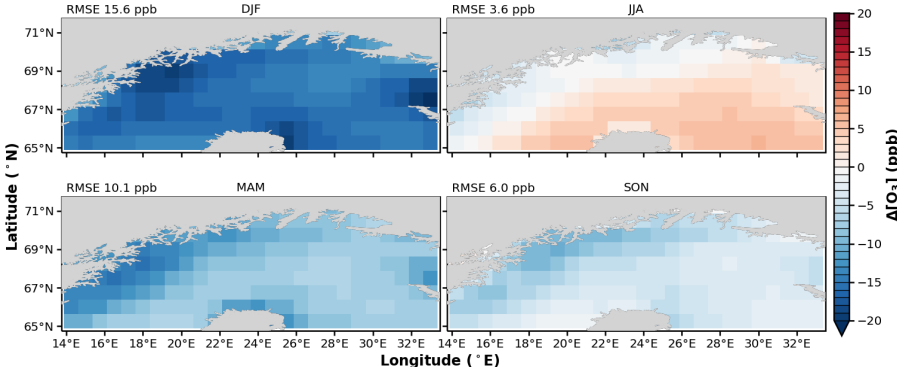


(b)

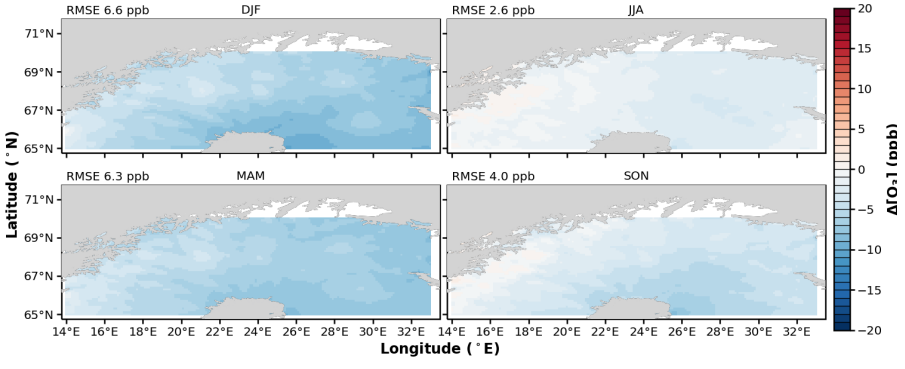


(c)

**Figure 4.** Divergence of reanalysis products from generalized ozone climatology for northern Fennoscandia: (a) MACC; (b) CAMS; (c) CAMSRAQ. Negative/positive values indicate that the reanalysis product underestimates/overestimates the tropospheric background $[O_3]$. Shown are seasonal averages: December/January/February (DJF); June/July/August (JJA); March/April/May (MAM); September/October/November (SON). The RMSE has been computed over land-only and is displayed in the upper left corner of each panel.

https://doi.org/10.5194/acp-2021-527
Preprint. Discussion started: 6 July 2021


Atmospheric Chemistry and Physics Discussions

The performance of CAMSRAQ ensemble and each of its contributing models is continuously validated with data from active European monitoring stations south of $60.53\,^{\circ}\mathrm{N}$. This validation is graphically provided on the Copernicus website (last accessed in May 2021). Following the Copernicus Atmosphere Monitoring Service (2020) guidelines, the analysis comprises mean bias, modified mean bias, RMSE, fractional gross error, and temporal correlations of the $\mathrm{O_3}$ daily maximum given in units of $\mu\,\mathrm{m}^{-3}$. All analyses are available for $\mathrm{O_3}$, nitrogen dioxide ($\mathrm{NO_2}$), and particular matter (PM) of $10\,\mu\mathrm{m}$ and $2.5\,\mu\mathrm{m}$ size. We multiply with a factor of $0.5$ to convert to units of $\mathrm{ppb}$. The ensemble median of the $\mathrm{O_3}$ daily maximum shows the largest RMSE in JJA ($5.28\,\mathrm{ppb}$) and the smallest in MAM ($4.05\,\mathrm{ppb}$) which is contrary to our results for the daily mean $\mathrm{O_3}$. The mean bias oscillates between $0.97\,\mathrm{ppb}$ (DJF) and $-1.77\,\mathrm{ppb}$ (JJA) which is opposite to our evaluation in northern Fennoscandia with a small bias in JJA and a larger negative deviation from observation in DJF and MAM. This indicates that CAMSRAQ might have different issues depending on the region of interest.

### 3.2 Reconstruction of missing ozone data

Based on our assessment, only the CAMSRAQ product suffices for gap-filling. We shall now derive a reconstruction method based on a Reynolds decomposition for use in ozone impact studies on vegetation. We will compare the reconstructed data with an evaluation of CAMSRAQ at the nearest neighboring grid point and compute the respective RSMEs with respect to observed data before and after the gap. The ozone data was taken at Svanvik in 2018. Due to problems in data acquisition, 9–23 July 2018 are missing from the record. These coincide with large, active forest fires in central Sweden (Björklund et al., 2019) which presumably caused elevated concentrations of ozone precursors. Enhanced $[\mathrm{O_3}]$ were observed throughout July and coincident peak concentrations above $40\,\mathrm{ppb}$ are found in the data series from Esrange and Pallas on July 4, 12–16, 25, and 31 (Fig. 6a). At Svanvik, the peak $[\mathrm{O_3}]$ in early July was not observed but elevated $[\mathrm{O_3}]$ occurred at the end of the month. During these forest fire-induced pollution events, $[\mathrm{O_3}]$ deviated from the respective climatology by up to $28\,\mathrm{ppb}$ (Fig. 6b). These special conditions demand a more elaborate gap-filling procedure than suggested by Mills et al. (2020).

A Reynolds decomposition is an analytical method often used in atmospheric and climate science to separate the expected value ($\bar{u}$) of a variable $u$ from its fluctuations ($u'$):

$$u = \bar{u} + u'. \tag{1}$$

As expected value, we assume the averaged seasonal cycle from a subset of ozone monitoring data excluding the year of interest and refer to this as ozone climatology $\langle[\mathrm{O_3}]\rangle$. The fluctuations $\Delta[\mathrm{O_3}]$ (anomalies) for the year of interest are derived in accordance to Eq. (1):

$$\Delta[\mathrm{O_3}] = \langle[\mathrm{O_3}]\rangle - [\mathrm{O_3}]. \tag{2}$$

To synchronize the time series temporally, we compute time-lagged correlations between Svanvik and the other stations in northern Fennoscandia during the overlapping periods in the 1990s (Fig. 5). To this end, we shift one series by $\Delta t$ and find the respective Pearson correlation coefficient. The data show a correlation maximum with Esrange and Pallas at $+3\,\mathrm{h}$ and $+1\,\mathrm{h}$ with Jergul/Karasjok. This means that these lag behind Svanvik. Of all stations, only Pallas displays a sufficiently high

https://doi.org/10.5194/acp-2021-527
Preprint. Discussion started: 6 July 2021


Atmospheric Chemistry and Physics Discussions

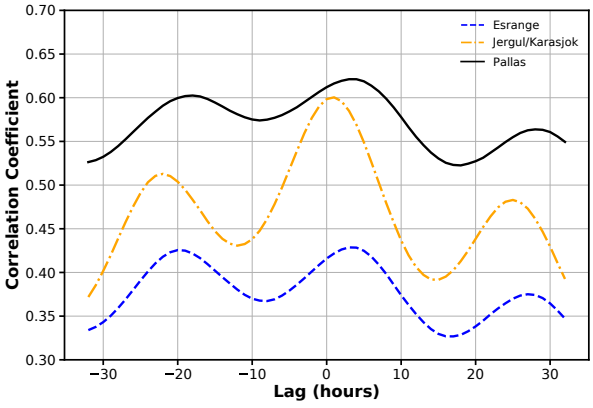


**Figure 5.** Temporal correlation of $[O_3]$ data between Svanvik and other ozone monitoring sites in northern Fennoscandia over time lag. The time lag correlation has been computed by shifting one of the series by $\Delta t$. A negative lag means that Svanvik lags behind, while a positive lag mean the other station lags behind. The highest correlation with Pallas/Esrange is found at a time lag of 3 h, for Jergul/Karasjok at 1 h.

correlation with Svanvik ($r^2 \geq 0.61$) (Mills et al., 2020, Section 12.5). We, therefore, choose Pallas as the reference station for the following reconstruction procedure. We derive a projection of the generalized ozone climatology to Svanvik and account for the time lag by shifting the climatology by 3 h:

$$P_{\text{Svanvik}} = \frac{\langle [O_3] \rangle^{\text{Svanvik}}_{\text{hourly}}}{\langle [O_3] \rangle_{\text{hourly, t'=t-3}}}. \tag{3}$$

We apply Eq. (2) to derive 1-hourly anomalies compared to the generalized climatology for each active station in 2018

$$\Delta [O_3]_{\text{hourly}}{}^{i} = [O_3]_{\text{hourly}}{}^{i} - \langle [O_3] \rangle_{\text{hourly}}, \tag{4}$$

with $i \in \{\text{Esrange, Pallas, Svanvik}\}$.

Observational data for Svanvik, Esrange, and Pallas for July 2018 is depicted in Fig. 6a. For reference, we overlay the generalized climatology, the climatology for Svanvik in 1-hourly resolution, and indicate the time-lag corrected generalized climatology.

We also correct the derived ozone anomalies at Pallas for the time lag $\Delta [O_3]^{\text{Pallas}}_{\text{hourly, t-3}}$ and use the projection (Eq. (3)) to reconstruct anomalies for the missing values at Svanvik:

$$\Delta [O_3]^{\text{Svanvik, reco}}_{\text{hourly}} = \Delta [O_3]^{\text{Pallas}}_{\text{hourly, t-3}} \cdot P_{\text{Svanvik}}. \tag{5}$$

The result is depicted in Fig. 6b, where the 1-hourly ozone concentration anomalies are shown together with the reconstructed anomalies for Svanvik. We do not account for the transport of pollutants or advection of ozone in our reconstruction procedure which results in a prominent lag between the reconstruction and the observations on July 25/26. In the context of risk assessment of ozone damage on vegetation, this has no large impact, as the applied flux-based metric $\text{POD}_y$ is usually integrated over a whole season (e.g. Mills et al., 2011).

https://doi.org/10.5194/acp-2021-527
Preprint. Discussion started: 6 July 2021


Atmospheric Chemistry and Physics Discussions

Finally, we add these anomalies to the Svanvik climatology, account for the estimated bias due to the change in tropospheric background ozone ($\delta[\mathrm{O_3}] = 1.2\,\mathrm{ppb}$), and derive the reconstructed time series

$$[\mathrm{O_3}]^{\mathrm{Svanvik,reco}}_{\mathrm{hourly}} = \langle[\mathrm{O_3}]\rangle^{\mathrm{Svanvik}}_{\mathrm{hourly}} + \Delta[\mathrm{O_3}]^{\mathrm{Svanvik,reco}}_{\mathrm{hourly}} + \delta[\mathrm{O_3}]. \tag{6}$$

In Fig. 6c), our reconstruction is shown together with the observed data before and after the gap and the CAMSRAQ evaluated at the nearest neighboring grid point. Both perform qualitatively well. To quantify the performance of our reconstruction and the CAMSRAQ, we compute RMSEs for the days in July for which observational data is available. We find an $\mathrm{RSME} = 5.89\,\mathrm{ppb}$ for our reconstruction and $\mathrm{RSME} = 7.34\,\mathrm{ppb}$ for the CAMSRAQ. This indicates that our reconstruction has an accuracy of about $78\,\%$ and is thus performing slightly better than CAMSRAQ ($73\,\%$) despite not accounting for atmospheric transport explicitly.

## 4 Conclusions

We derived a representative ozone climatology for northern Fennoscandia based on long-term ground-level ozone monitoring in northern Finland, Norway, and Sweden. Based on this generalized ozone climatology, we assessed the quality of available global (MACC and CAMSRA) and regional (CAMSRAQ) reanalysis products for northern Fennoscandia focussing on the seasonality of ozone. We confirm previously published results concerning the quality of global reanalysis products (Huijnen et al., 2020; Barten et al., 2020) and find that the observed ozone patterns in northern Fennoscandia are not reproduced well. Better performance was displayed by the regional model reanalysis CAMSRAQ ensemble which reproduces the observed ozone seasonality well, although with a remaining average deviation of up to $-7\,\mathrm{ppb}$. All products showed deficits, in particular during winter and spring. We confirm that a high spatial and temporal resolution, state-of-the-art mechanistic removal processes (land–atmosphere–ocean), and assimilation of in situ observations at ground-level are a must to constrain reanalysis products, especially at high latitudes during times when the coverage by passive sounders onboard satellites is low.

There is a multitude of probable reasons for the differences found between the reanalysis products and observations. The enhancements which led from the MACC reanalysis to CAMSRA have been reported and discussed by Inness et al. (2019) on global scales. Amongst others, assimilation of ozone profiles from satellite retrieval (compared to column densities) and an upgraded ozone chemistry have led to an enhanced performance of CAMSRA, but a considerable bias remains (Huijnen et al., 2020). In particular, Barten et al. (2020) reported a pronounced underestimation for CAMSRA in the high Arctic (e.g., Summit, Greenland) and attribute this to an insufficient representation of a mechanistic dry deposition scheme to the ocean. The large divergence which we found in all seasons but summer either points to a deficit in modeled removal processes or too weak model constraints by data from passive sounders onboard satellites in polar winter. In particular, too high dry deposition velocities over snow and ice-covered surfaces would not allow for a sufficient build-up of ozone and precursors in winter leading to too low modeled ozone concentrations (Falk and Sinnhuber, 2018; Falk and Søvde Haslerud, 2019). Due to the higher spatial resolution of the regional air quality models, CAMSRAQ is capable of capturing small-scale depletion and peak episodes of ozone. The higher spatial and temporal resolution improves daily and seasonal cycles of modeled ozone which

https://doi.org/10.5194/acp-2021-527
Preprint. Discussion started: 6 July 2021


Atmospheric Chemistry and Physics Discussions

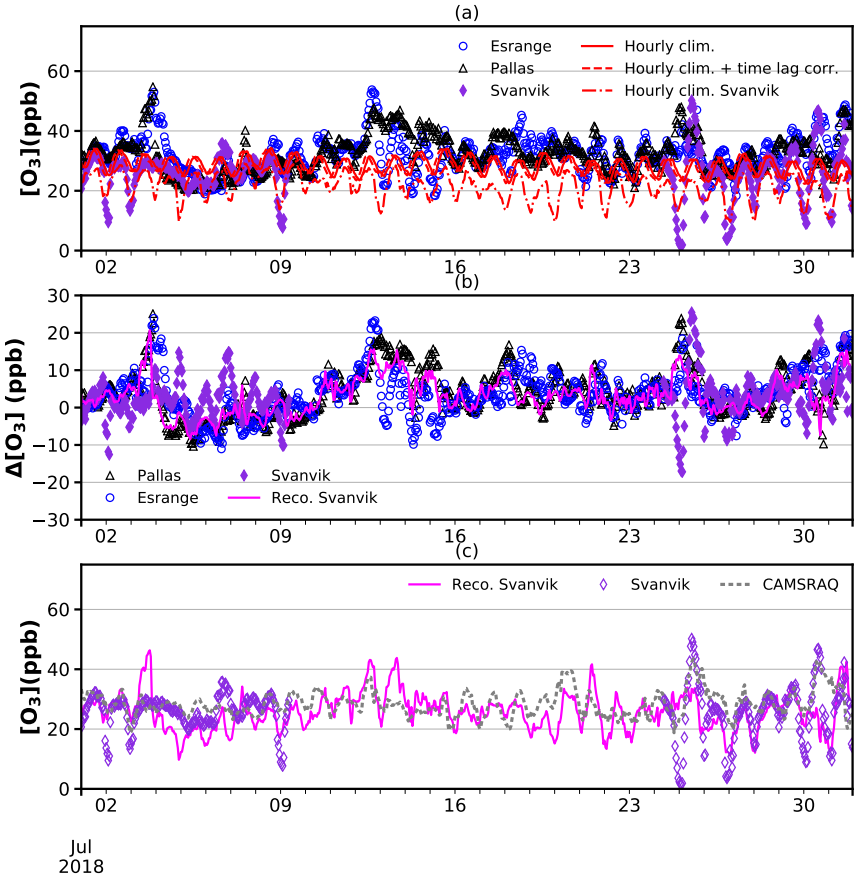


**Figure 6.** Reconstruction procedure for missing $[O_3]$ data (July 9–23, 2018). Observed 1-hourly $[O_3]$ are shown together with 1-hourly climatologies derived for northern Fennoscandia (combined data from Esrange, Jergul/Karasjok, Pallas) and Svanvik. (a) Time series supplemented with 1-hourly climatologies. The time-lag correction of the northern Fennoscandia climatology is also indicated; (b) observed and reconstructed anomalies; (c) reconstructed $[O_3]$ for Svanvik in comparison with CAMSRAQ evaluated at the nearest neighboring grid point.

is especially important for the use in risk assessment for vegetation damage and human health. Improvements in atmospheric transport as part of the OpenIFS updates may play also a role but cannot be assessed from our analysis. The higher spatial and temporal resolution of CAMSRAQ aside, we can assume the assimilated ground-level ozone data was another driver for the different performance as passive sounders onboard satellites typically resolve $[O_3]$ at the surface rather poorly and hence do not constrain the global models well enough (Andersson et al., 2017).

To account for missing data from the 2018 record at Svanvik located in northern Norway in July, we proposed a routine for reconstruction of 1-hourly ozone data adhering to the UNECE-LRTAP conventions (Mills et al., 2020). We performed a Reynolds decomposition into anomalies and climatology, identified a reference station with the highest Pearson correlation coefficient, synchronized the time series using a time lag correlation, and corrected for a bias induced by the increase in

https://doi.org/10.5194/acp-2021-527
Preprint. Discussion started: 6 July 2021


Atmospheric Chemistry and Physics Discussions

tropospheric background ozone concentrations since the end of the regular data taking at Svanvik in the mid-1990s. As we don't take atmospheric transport of pollutants into account, the reconstructed data display inaccuracies in the timing of peak episodes. This deficit, however, has no large impact in the context of risk assessment of ozone damage on vegetation because the applied flux-based metrics typically integrate the ozone uptake over a whole season. Our devised reconstruction method performs better (78 % accuracy) than evaluating CAMSRAQ at the nearest neighboring grid point. However, two criteria have to be met before our reconstruction can be performed: 1. Availability of overlapping long-term series. 2. Availability of overlapping data from a reasonably close-by site with a high Pearson correlation coefficient during the occurrence of the gap.

In summary, we can recommend using the CAMSRAQ for gap-filling of ozone monitoring data in northern Fennocandia if no other means of reconstruction are available. We strongly advise against using any of the global reanalysis products (MACC, CAMSRA) for this purpose.

*Code availability.* Python 2.7 code is available under Common Creative Licence on the GitHub repository of the corresponding author. Please get in touch for further information.

*Data availability.* All observational data is available form NILU's EBAS database. MACC and CAMS reanalysis data is available through ECMWF's data services. CAMSRAQ is available from the regional atmosphere data service of copernicus.

*Author contributions.* SF aquired and processed all data, conducted the analysis, and composed the figures and manuscript. AVV and FS contributed to proofreading. All authors contributed to discussion.

*Competing interests.* The authors declare that they have no conflict of interest.

*Acknowledgements.* This work was funded by the Norwegian Research Council (NRC) through the project The double punch: Ozone and climate stresses on vegetation (268073). We would also like to thank the LATICE research group and the EMERALD project (294948) for supporting this work.

https://doi.org/10.5194/acp-2021-527
Preprint. Discussion started: 6 July 2021


Atmospheric Chemistry and Physics Discussions

## References

Ainsworth, E. A.: Understanding and improving global crop response to ozone pollution, Plant J., 90, 886–897, https://doi.org/10.1111/tpj.13298, 2017.

Andersson, C., Alpfjord, H., Robertson, L., Karlsson, P. E., and Engardt, M.: Reanalysis of and attribution to near-surface ozone concentrations in Sweden during 1990–2013, Atmospheric Chemistry and Physics, 17, 13 869–13 890, https://doi.org/10.5194/acp-17-13869-2017, 2017.

Barten, J. G. M., Ganzeveld, L. N., Steeneveld, G.-J., and Krol, M. C.: Role of oceanic ozone deposition in explaining short-term variability of Arctic surface ozone, Atmospheric Chemistry and Physics Discussions, 2020, 1–28, https://doi.org/10.5194/acp-2020-978, 2020.

Björklund, J.-Å., Ekelund, K., Henningsson, A., Perers, K., Peters, J., Siverstig, A., Uddholm, L.-G., and Wisén, J.: Betänkande av 2018 års skogsbrandsutredning, SOU2019 7, Statens Offentliga Utredningar (SOU), https://www.regeringen.se/rattsliga-dokument/statens-offentliga-utredningar/2019/02/sou-20197/, 2019.

Chuwah, C., van Noije, T., van Vuuren, D. P., Stehfest, E., and Hazeleger, W.: Global impacts of surface ozone changes on crop yields and land use, Atmos. Environ., 106, 11–23, https://doi.org/10.1016/j.atmosenv.2015.01.062, 2015.

Clifton, O., Fiore, A., Massman, W., Baublitz, C., Coyle, M., Emberson, L., Fares, S., Farmer, D., Gentine, P., Gerosa, G., Guenther, A., Helmig, D., Lombardozzi, D., Munger, J., Patton, E., Pusede, S., Schwede, D., Silva, S., Sörgel, M., and Tai, A.: Dry Deposition of Ozone Over Land: Processes, Measurement, and Modeling, Reviews of Geophysics, p. e2019RG000670, https://doi.org/10.1029/2019RG000670, 2020.

Copernicus Atmosphere Monitoring Service: Verification plots: documentation, http://macc-raq-op.meteo.fr/doc/USER_GUIDE_VERIFICATION_STATISTICS.pdf, 2020.

Emberson, L.: Effects of ozone on agriculture, forests and grasslands, Philosophical transactions. Series A, Mathematical, physical, and engineering sciences, 378, 20190 327, https://doi.org/10.1098/rsta.2019.0327, 2020.

Falk, S. and Sinnhuber, B.-M.: Polar boundary layer bromine explosion and ozone depletion events in the chemistry-climate model EMAC v2.52: implementation and evaluation of AirSnow algorithm, Geosci. Model Dev., 11, 1115–1131, https://doi.org/10.5194/gmd-11-1115-2018, 2018.

Falk, S. and Søvde Haslerud, A.: Update and evaluation of the ozone dry deposition in Oslo CTM3 v1.0, Geosci. Model Dev., 12, 4705–4728, https://doi.org/10.5194/gmd-12-4705-2019, 2019.

Fleming, Z. L., Doherty, R. M., von Schneidemesser, E., Malley, C. S., Cooper, O. R., Pinto, J. P., Colette, A., Xu, X., Simpson, D., Schultz, M. G., Lefohn, A. S., Hamad, S., Moolla, R., Solberg, S., and Feng, Z.: Tropospheric Ozone Assessment Report: Present-day ozone distribution and trends relevant to human health, Elementa-Sci Anthrop., 6, https://doi.org/10.1525/elementa.273, 2018.

Franz, M. and Zaehle, S.: Competing effects of nitrogen deposition and ozone exposure on northern hemispheric terrestrial carbon uptake and storage, 1850–2099, Biogeosciences, 18, 3219–3241, https://doi.org/10.5194/bg-18-3219-2021, 2021.

Hatakka, J., Aalto, T., Aaltonen, V., Aurela, M., Hakola, H., Komppula, M., Laurila, T., Lihavainen, H., Paatero, J., Salminen, K., and Viisanen, Y.: Overview of the atmospheric research activities and results at Pallas GAW station, Boreal Environ. Res., 8, 365–383, 2003.

Høgda, K., Tømmervik, H., and Karlsen, S.: Trends in the Start of the Growing Season in Fennoscandia 1982-2011, Remote Sens., 5, 4304–4318, https://doi.org/10.3390/rs5094304, 2013.

Hoshika, Y., Katata, G., Deushi, M., Watanabe, M., Koike, T., and Paoletti, E.: Ozone-induced stomatal sluggishness changes carbon and water balance of temperate deciduous forests, Sci. Rep.-UK, 5, https://doi.org/10.1038/srep09871, 2015.

https://doi.org/10.5194/acp-2021-527
Preprint. Discussion started: 6 July 2021


Atmospheric Chemistry and Physics Discussions

Huijnen, V., Miyazaki, K., Flemming, J., Inness, A., Sekiya, T., and Schultz, M. G.: An intercomparison of tropospheric ozone reanalysis products from CAMS, CAMS interim, TCR-1, and TCR-2, Geosci. Model Dev., 13, 1513–1544, https://doi.org/10.5194/gmd-13-1513-2020, 2020.

Inness, A., Baier, F., Benedetti, A., Bouarar, I., Chabrillat, S., Clark, H., Clerbaux, C., Coheur, P., Engelen, R., Errera, Q., Flemming, J., George, M., Granier, C., Hadji-Lazaro, J., Huijnen, V., Hurtmans, D., Jones, L., Kaiser, J., Kapsomenakis, J., and Zerefos, C.: The MACC reanalysis: An 8 yr data set of atmospheric composition, Atmos. Chem. Phys., 13, 4073–4109, https://doi.org/10.5194/acp-13-4073-2013, 2013.

Inness, A., Ades, M., Agusti-Panareda, A., Barré, J., Benedictow, A., Blechschmidt, A.-M., Dominguez, J., Engelen, R., Eskes, H., Flemming, J., Huijnen, V., Jones, L., Kipling, Z., Massart, S., Parrington, M., Peuch, V.-H., Razinger, M., Rémy, S., Schulz, M., and Suttie, M.: The CAMS reanalysis of atmospheric composition, Atmos. Chem. Phys., 19, 3515–3556, https://doi.org/10.5194/acp-19-3515-2019, 2019.

Kangaskärvi, J., Jaspers, P., and Kollist, H.: Signalling and cell death in ozone-exposed plants, Plant, Cell & Environment, 28, 1021–1036, https://doi.org/10.1111/j.1365-3040.2005.01325.x, 2005.

Karlsen, S., Solheim, I., Beck, P., Høgda, K., Wielgolaski, F., and Tømmervik, H.: Variability of the start of the growing season in Fennoscandia, 1982–2002, Int. J. Biometeorol., 51, 513–24, https://doi.org/10.1007/s00484-007-0091-x, 2007.

Karlsson, P., Ferm, M., Tømmervik, H., Hole, L., Karlsson, G., Ruoho-Airola, T., Aas, W., Hellsten, S., Akselsson, C., Mikkelsen, T., and Nihlgård, B.: Biomass burning in eastern Europe during spring 2006 caused high deposition of ammonium in northern Fennoscandia, Environ. Pollut., 176C, 71–79, https://doi.org/10.1016/j.envpol.2012.12.006, 2013.

Karlsson, P. E., Pleijel, H., Andersson, C., Bergström, R., Engardt, M., Eriksen, A., Falk, S., Klingberg, J., Langner, J., Manninen, S., Stordal, F., Tømmervik, H., and Vollsnes, A.: The vulnerability of northern European vegetation to ozone damage in a changing climate - An assessment based on current knowledge, Tech. Rep. C586, IVL Svenska Miljöinstitutet, https://www.ivl.se/publikationer/publikation.html?id=6220, 2021.

Linderholm, H.: Growing Season Changes in the Last Century, Agr. Forest Meteorol., 137, 1–14, https://doi.org/10.1016/j.agrformet.2006.03.006, 2006.

Lindskog, A., Karlsson, P., Grennfelt, P., Solberg, S., and Forster, C.: An exceptional ozone episode in northern Fennoscandia, Atmos. Environ., 41, 950–958, https://doi.org/10.1016/j.atmosenv.2006.09.027, 2007.

Lombardozzi, D., Bonan, G. B., Smith, N. G., Dukes, J. S., and Fisher, R. A.: Temperature acclimation of photosynthesis and respiration: A key uncertainty in the carbon cycle-climate feedback, Geophys. Res. Lett., 42, 8624–8631, https://doi.org/10.1002/2015GL065934, 2015a.

Lombardozzi, D., Levis, S., Bonan, G., Hess, P., and Sparks, J.: The Influence of Chronic Ozone Exposure on Global Carbon and Water Cycles, J. Climate, 28, 292–305, https://doi.org/10.1175/JCLI-D-14-00223.1, 2015b.

Mills, G., Hayes, F., Simpson, D., Emberson, L., Norris, D., Harmens, H., and Büker, P.: Evidence of widespread effects of ozone on crops and (semi-)natural vegetation in Europe (1990–2006) in relation to AOT40- and flux-based risk maps, Glob. Change Biol., 17, 592 – 613, https://doi.org/10.1111/j.1365-2486.2010.02217.x, 2011.

Mills, G., Sharps, K., Simpson, D., Pleijel, H., Broberg, M., Uddling, J., Jaramillo, F., Davies, W. J., Dentener, F., Van den Berg, M., Agrawal, M., Agrawal, S. B., Ainsworth, E. A., Büker, P., Emberson, L., Feng, Z., Harmens, H., Hayes, F., Kobayashi, K., Paoletti, E., and Van Dingenen, R.: Ozone pollution will compromise efforts to increase global wheat production, Glob. Change Biol., 24, 3560–3574, https://doi.org/10.1111/gcb.14157, 2018.

https://doi.org/10.5194/acp-2021-527
Preprint. Discussion started: 6 July 2021


Atmospheric Chemistry and Physics Discussions

Mills, G., Pleijel, H., Malley, C. S., Sinha, B., Cooper, O. R., Schultz, M. G., Neufeld, H. S., Simpson, D., Sharps, K., Feng, Z., Gerosa, G., Harmens, H., Kobayashi, K., Saxena, P., Paoletti, E., Sinha, V., and Xu, X.: Tropospheric Ozone Assessment Report: Present-day tropospheric ozone distribution and trends relevant to vegetation, Elementa-Sci Anthrop., 6, https://doi.org/10.1525/elementa.302, 2018.

Mills, G., Harmens, H., Hayes, F., Pleijel, H., Büker, P., González-Fernandéz, I., Alonso, R., Hayes, F., and Sharps, K.: SCIENTIFIC BACKGROUND DOCUMENT B - DEVELOPING AREAS OF RESEARCH OF RELEVANCE TO CHAPTER III (MAPPING CRITICAL LEVELS FOR VEGETATION) OF THE MODELLING AND MAPPING MANUAL OF THE LRTAP CONVENTION, International Cooperative Programme on Effects of Air Pollution on Natural Vegetation and Crops, https://icpvegetation.ceh.ac.uk/sites/default/files/Scientific%20Background%20document%20B%20June%202020.pdf, 2020.

Monks, P. S.: A review of the observations and origins of the spring ozone maximum, Atmos. Environ., 34, 3545–3561, https://doi.org/10.1016/S1352-2310(00)00129-1, 2000.

Monks, P. S., Archibald, A. T., Colette, A., Cooper, O., Coyle, M., Derwent, R., Fowler, D., Granier, C., Law, K. S., Mills, G. E., Stevenson, D. S., Tarasova, O., Thouret, V., von Schneidemesser, E., Sommariva, R., Wild, O., and Williams, M. L.: Tropospheric ozone and its precursors from the urban to the global scale from air quality to short-lived climate forcer, Atmos. Chem. Phys., 15, 8889–8973, https://doi.org/10.5194/acp-15-8889-2015, 2015.

Myhre, G., Shindell, D., Bre´on, F.-M., Collins, W., Fuglestvedt, J., Huang, J., Koch, D., Lamarque, J.-F., Lee, D., Mendoza, B., Nakajima, T., Robock, A., Stephens, G., Takemura, T., and Zhang, H.: Anthropogenic and Natural Radiative Forcing, book section 8, p. 659–740, Cambridge University Press, Cambridge, United Kingdom and New York, NY, USA, https://doi.org/10.1017/CBO9781107415324.018, 2013.

Pellegrini, E., Francini, A., Lorenzini, G., and Nali, C.: PSII photochemistry and carboxylation efficiency in Liriodendron tulipifera under ozone exposure, Environ. Exp. Bot., 70, 217–226, 2011.

Solberg, S.: Monitoring of boundary layer ozone in Norway from 1977 to 2002, Ozone Report 2003 85, Norwegian Institute for Air Research (NILU), 2003.

Stevenson, D. S., Dentener, F. J., Schultz, M. G., Ellingsen, K., van Noije, T. P. C., Wild, O., Zeng, G., Amann, M., Atherton, C. S., Bell, N., Bergmann, D. J., Bey, I., Butler, T., Cofala, J., Collins, W. J., Derwent, R. G., Doherty, R. M., Drevet, J., Eskes, H. J., Fiore, A. M., Gauss, M., Hauglustaine, D. A., Horowitz, L. W., Isaksen, I. S. A., Krol, M. C., Lamarque, J.-F., Lawrence, M. G., Montanaro, V., Müller, J.-F., Pitari, G., Prather, M. J., Pyle, J. A., Rast, S., Rodriguez, J. M., Sanderson, M. G., Savage, N. H., Shindell, D. T., Strahan, S. E., Sudo, K., and Szopa, S.: Multimodel ensemble simulations of present-day and near-future tropospheric ozone, J. Geophys. Res.-Atmos., 111, https://doi.org/10.1029/2005JD006338, 2005.

Tai, A. P. K., Martin, M. V., and Heald, C. L.: Threat to future global food security from climate change and ozone air pollution, Nat. Clim. Change, 4, 817–821, https://doi.org/10.1038/NCLIMATE2317, 2014.

Tang, H., Takigawa, M., Liu, G., Zhu, J., and Kobayashi, K.: A projection of ozone-induced wheat production loss in China and India for the years 2000 and 2020 with exposure-based and flux-based approaches, Glob. Change Biol., 19, 2739–2752, https://doi.org/10.1111/gcb.12252, 2013.

Škerlak, B., Sprenger, M., Pfahl, S., Tyrlis, E., and Wernli, H.: Tropopause folds in ERA-Interim: Global climatology and relation to extreme weather events, J. Geophys. Res.-Atmos., 120, 4860–4877, https://doi.org/10.1002/2014JD022787, 2015.

Watanabe, M., Hoshika, Y., and Koike, T.: Photosynthetic responses of Monarch birch seedlings to differing timings of free air ozone fumigation, J. Plant Res., 127, 339–345, https://doi.org/10.1007/s10265-013-0622-y, 2014.

WHO - World Health Organization: Health risks of ozone from long-range transboundary air pollution, 2008.

https://doi.org/10.5194/acp-2021-527
Preprint. Discussion started: 6 July 2021


Atmospheric Chemistry and Physics Discussions

Young, P. J., Archibald, A. T., Bowman, K. W., Lamarque, J.-F., Naik, V., Stevenson, D. S., Tilmes, S., Voulgarakis, A., Wild, O., Bergmann, D., Cameron-Smith, P., Cionni, I., Collins, W. J., Dalsøren, S. B., Doherty, R. M., Eyring, V., Faluvegi, G., Horowitz, L. W., Josse, B., Lee, Y. H., MacKenzie, I. A., Nagashima, T., Plummer, D. A., Righi, M., Rumbold, S. T., Skeie, R. B., Shindell, D. T., Strode, S. A., Sudo, K., Szopa, S., and Zeng, G.: Pre-industrial to end 21st century projections of tropospheric ozone from the Atmospheric Chemistry and Climate Model Intercomparison Project (ACCMIP), Atmos. Chem. Phys., 13, 2063–2090, https://doi.org/10.5194/acp-13-2063-2013, 2013.

Zhu, J., Tai, A. P. K., and Yim, S. H. L.: Effects of ozone-vegetation interactions on meteorology and air quality in China using a two-way coupled land-atmosphere model, Atmospheric Chemistry and Physics Discussions, 2021, 1–23, https://doi.org/10.5194/acp-2021-165, 2021.